136 (2022) 212763

Contents lists available at ScienceDirect

Biomaterials Advances

journal homepage: www.journals.elsevier.com/materials-science-and-engineering-c

Surface modified hexagonal upconversion nanoparticles for the development of competitive assay for biodetection

Padmaja Parameswaran Nampi [a,b,c,*,1,2], Alexander Vakurov [b,1], Sikha Saha [c,2], Gin Jose [a,2], Paul A. Millner [b]

[a] School of Chemical and Process Engineering, Faculty of Engineering and Physical Sciences, University of Leeds, Leeds LS2 9JT, United Kingdom
[b] School of Biomedical Sciences, Faculty of Biological Sciences, University of Leeds, Leeds LS2 9JT, United Kingdom
[c] Leeds Institute of Cardiovascular and Metabolic Medicine (LICAMM), Faculty of Medicine and Health, University of Leeds, Leeds LS2 9JT, United Kingdom

ARTICLE INFO

Keywords:
Up-conversion nanoparticles
Photoluminescence
Detection
Ofloxacin
Competitive assay

ABSTRACT

Up-conversion nanoparticles (UCNPs) of sodium yttrium fluoride with ytterbium and erbium ions as sensitizer and activator (β-$NaYF_4$/Yb^{3+}/Er^{3+}) have been synthesised by a solvothermal method. The synthesised particles were found to be highly uniform in size (~50 nm) and of hexagonal crystal phase producing strong up-conversion luminescence dominated in the green wavelength region. During the synthesis, photoluminescence properties of the reaction mixture were monitored at regular intervals to ensure the required particle size distribution and luminescence efficiency. The hydrophobic particles thus obtained were modified by coating with silica, yielding particles that were stable in aqueous media. The silica coated UCNPs were further modified with maleimide-polyethylene glycol-silane (mal-PEG-silane) to provide thiol reactive surface groups. The silanized, maleimide-bearing UCNPs were effective for conjugating to reductively-cleaved half antibodies against ofloxacin, a veterinary antibiotic, to produce photoluminescent nanobiosensors for its detection and quantification. The speed and minimum detection concentration (~10 nM) that we report for a competitive assay of ofloxacin in this study is promising for developing sensors for this and other biomolecules.

1. Introduction

Up-conversion is a process whereby near-infrared (NIR) or infrared (IR) light, is converted to higher energy, ultraviolet (UV) or visible light, via multiple photon absorption and energy transfer in rare earth doped materials [1,2]. Up-conversion nanoparticles (UCNPs) with good photoluminescence efficiency have been recognised as suitable for bio-labelling applications [3,4]. For efficient bio-detection, engineering of UCNPs with uniform shape and size and high photoluminescence (PL) yield is essential. UCNPs are generally comprised of inorganic nanoparticles doped with sensitizer and activator rare earth ions. The efficiency of up-conversion emission can be improved by promoting the energy transfer between the sensitizer and the activator with the assistance of the host lattice [2]. The sensitizer chosen should have good absorption cross-section to absorb the energy from the excitation light, usually a laser, and the host should mediate transfer of this energy to the activator, mainly through non-radiative and phonon assisted processes. To date, efficient up-conversion emission with good potential for biosensing and imaging applications has only been observed in a very few dopant-host combinations, such as $NaYF_4$:Yb^{3+}/Er^{3+} [3,5]. However, the up-conversion luminescence efficiency is also nanoparticle size-dependent due to decreasing number of emitting ions and increasing surface-to-volume ratio leading to stronger surface quenching effects at smaller particle diameters [6–9]. The non-radiative deactivation channels are believed to be related to the surface properties of the nanoparticles. These size dependency on photoluminescence are mainly due to such phonon-mediated energy transfer processes [10] and are effected by high energy vibrations of ligands, surfactants [6] and surrounding solvents [8] containing –OH and -CH groups [8], from increased surface defect density [8] or from a combination of these effects. There are reports on the dependence of shape on luminescent properties in oxide nanoparticles [11,12].

* Corresponding author at: School of Chemical and Process Engineering, Faculty of Engineering and Physical Sciences, University of Leeds, Leeds LS2 9JT, United Kingdom.
E-mail address: p.nampi@leeds.ac.uk (P.P. Nampi).
[1] Contributed to the work equally.
[2] Associated with Bragg Centre for Materials Research, University of Leeds, United Kingdom.

https://doi.org/10.1016/j.bioadv.2022.212763
Received 12 November 2021; Received in revised form 3 March 2022; Accepted 13 March 2022
Available online 17 March 2022

The highest up-conversion efficiencies observed have been in hexagonal phase $NaYF_4$ bulk materials doped with the Er^{3+}/Yb^{3+} or Tm^{3+}/Yb^{3+} ions synthesised using solid-state methods [13,14]. Colloidal nanosuspensions of upconverting $NaYF_4$ nanocrystals, and related materials, have also been synthesised through various protocols including thermal decomposition, precipitation, and high-pressure reactions [5,15–18]. Among many methods of synthesis of UCNPs, the solvothermal reaction with a high boiling point solvent was successful in preparing UCNPs with high up-conversion efficiency [19–21]. However, the colloidal nanoparticles thus produced, due to their hydrophobicity and need for organic solvents, were not suitable for many biological applications. To overcome this, the particles were surface engineered to convert them to be hydrophilic as well as chemically reactive. Reactive functional groups such as amines and thiols, allow attachment of specific biomolecules such as antibodies and enzymes. Methods such as ligand exchange, removal and oxidation, layer-by-layer assembly and surface silanization are the most prominent surface modification strategies reported [22]. However, ligand exchange was found to have an adverse effect on the resultant nanoparticle quality [23]. In contrast, a uniform surface layer of silica does not significantly change the PL emission properties of the UCNPs, but in addition, enhances their aqueous dispersibility, reduces the tendency for aggregation and significantly diminishes nonspecific binding in assays [24–27]. In this research, we have synthesised photoluminescent hexagonal crystal phased β $NaYF_4/Yb^{3+}/Er^{3+}$ UCNPs using a solvothermal method in oleic acid and 1-octadecene. A silica coating procedure was employed to improve the dispersibility of UCNPs in water and also for low cytotoxicity and provide a surface for further modification with different functional groups for effective attachment of antibodies. The silica coating created on the surface rendered the UCNPs hydrophilic and further addition of maleimide polyethylene glycol-silane (mal-PEG-silane) introduced maleimide groups which show specific reactivity with –SH groups. We used such modified nanoparticles to attach anti-ofloxacin half-antibodies. Ofloxacin is a commonly used veterinary antibiotic within the fluoroquinolone family currently causing environmental concerns and for which a rapid detection assay would be highly useful.

Usage of ofloxacin, a veterinary drug has benefited the animal industry and helped providing affordable animal proteins to the growing human population. However, its extensive use has led to worldwide concern due to its potential threat to human health by entering the food chain and contributing to bacterial resistance. In order to minimize the risk to human health via the development of bacterial resistance, analytical determination of ofloxacin is critical [28,29]. Several methods such as chemiluminescence [30], spectrophotometric methods [31], high performance liquid chromatography (HPLC) [32] and capillary electrophoresis [33] have been utilised for the detection of ofloxacin. But, most of these methods have the shortcoming of the need for extensive technology and poor detection limits in the mg/mL range. As low concentration of antibiotic residues might already select for resistant bacteria, development of sensitive and accurate detection methods capable of measuring low concentration of antibiotic residues should be developed. Hence, in the present study, ofloxacin was selected as the target analyte molecule in order to assess the suitability of our newly designed UCNP based nanobiosensor platform. The method of evaluation of the sensing adopting a competitive assay is found to be a single step procedure of using the ofloxacin modified 96 well plates and photoluminescent UCNPs are highly effective in the detection due to high signal/noise ratio.

2. Materials and methods

2.1. Materials

Chemicals such as sodium hydroxide (NaOH) (99%), yttrium (III) chloride hexahydrate ($YCl_3{\cdot}6H_2O$) (99.9%), ytterbium (III) chloride hexahydrate ($YbCl_3{\cdot}6H_2O$) (99.9%), erbium (III) chloride hexahydrate ($ErCl_3{\cdot}6H_2O$) (99.9%), oleic acid (Cat. W281506), 1-octadecene (>95%), ammonium fluoride (NH_4F) (99.5%), ammonia solution (30%), cyclohexane (99.5%), tetraethoxysilane (TEOS), IGEPAL CO-520 (IGEPAL), tris (2-carboxyethyl) phosphine hydrochloride (TCEP), bovine serum albumin (BSA), ethylenediamine, 1-ethyl-3-(-3-dimethylaminopropyl) carbodiimide hydrochloride (EDC), ofloxacin, sulfamethazine, acetone, methanol, Tween-20, phosphate buffer saline (PBS), nitrocellulose membrane and ECL chemiluminescence kit from Sigma-Aldrich were used in this research. The 4-(2-hydroxyethyl)-1-piperazineethanesulfonic acid (HEPES) buffer and N-hydroxysulfosuccinimide (Sulfo NHS) purchased from ThermoFisher Scientific have been utilised in the present study. Maleimide-PEG silane (mal-PEG-silane) from Creative PEG Networks, North Carolina, USA and rabbit anti-ofloxacin antibodies produced by Antibody Production Services of Life Science Group Ltd., UK, were used in this study. The antibodies were affinity purified before further use.

2.2. Synthesis and characterization of β $NaYF_4/Yb^{3+}/Er^{3+}$ up-conversion nanoparticles (UCNPs)

Hexagonal $NaYF_4/20\%Yb^{3+}/2\%Er^{3+}$ UCNPs were prepared by a modified solvothermal method reported by Plohl et al. [34]. In our experiment, 3.12 mmol of $YCl_3.6H_2O$, 0.8 mmol $YbCl_3.6H_2O$ and 0.08 mmol $ErCl_3.6H_2O$ were mixed with 24 mL oleic acid (OA) and 60 mL 1-octadecene (ODE) in a 250 mL five necked glass reaction vessel under Ar atmosphere. Oleic acid is the coordinating solvent while the non-coordinating solvent 1-octadecene was used as the primary solvent due to its high boiling point (315 °C). The solution was heated to a temperature of 200 °C to get a homogeneous mixture of rare earth chlorides in OA/ODE. This chloride precursor solution was then cooled down to a temperature of 65 °C and, 16 mmol of NH_4F and 10 mmol of NaOH dissolved in 20 mL of methanol were added. The temperature of the solution was then increased gradually to 300°C and maintained at this temperature for 2 h under Ar gas atmosphere and reflux conditions. Such higher reaction temperature and longer reaction time are required to provide sufficient free energy to overcome the activation barrier of an α/β phase transition [17,35]. In order to monitor the growth of particles and their rate of formation, a small quantity of the reaction mixture was taken at regular intervals, after 300°C, using microbore polytetrafluoroethylene (PTFE) tubing attached to a syringe and the upconversion PL spectrum and TEM have been taken. The final solution taken after 120 min was cooled to room temperature and the nanocrystals were separated by centrifuging the fine suspension at 80,000 g for 1 h using a Beckman Avanti J20XP high-speed centrifuge with the Beckman type 50.2 Ti rotor. The precipitate was washed four times with cyclohexane by dispersing and centrifuging at 80,000 g and redispersing the nanoparticle pellet in cyclohexane. The concentration of the UCNP suspension was found to be 60 mg/mL. The shape and size of particles present in solutions taken at different times were also studied. The particles are highly stable and the photoluminescence is not quenched even after several months.

Sizing of the particles was carried out by recording their TEM image on a JEOL-JEM1400 Transmission Electron Microscope. The samples for TEM were prepared by placing a drop of UCNP suspension in cyclohexane onto the surface of a holey carbon coated Cu grid and letting the solvent to vaporise prior to imaging. The size-distributions of nanoparticles were estimated from TEM images using ImageJ software; typically, at least 100 particles were measured. To assess photoluminescence, the sample solutions were irradiated with a 976 nm near-infrared laser (BL976-PAG900, Thorlabs) and UCNP emission recorded with a spectrometer (QE-PRO, Ocean Optics) with 5 s integration time and 1000 mA laser diode current. The powder X-ray diffraction (XRD) pattern of the UCNP sample (at 90 and 120 min reaction time) were obtained by a PANalytical X-Pert Pro Multipurpose Diffractometer. The diffraction patterns were acquired by irradiating the powder samples with Cu Kα radiation of 1.5406 Å wavelength with accelerating voltage

and emission current of 40 kV and 40 mA, respectively. Data were collected at a rate of 4°/min in the 2θ range from 10° to 80°.

2.3. Silica coating of UCNPs and functionalisation with mal-PEG-silane

Silica coating on the particle surface was carried out by a modified procedure as reported by Zhang et al. [36]. One millilitre of the nanoparticle suspension was mixed with 500 μL of IGEPAL and 50 mL of cyclohexane by ultrasonication for a period of 2 min followed by stirring for a period of 10 to 15 min. Ammonia solution (400 μL of 30% v/v in water) mixed with 2 mL of IGEPAL was then added to the above mixture followed by sonication for 30 s and stirring for 30 min. Tetraethoxysilane (TEOS) (200 μL) was added to this mixture and allowed to stir for a period of 48 h at room temperature to produce silica coated UCNPs. The silica coated UCNPs were separated from the solution by centrifugation at 80,000 g using a Beckman Avanti J20XP high-speed centrifuge (Beckman type 50.2 Ti rotor). The precipitate was then washed with 1:1 v/v EtOH/water and then redispersed in deionised water to a concentration of 8.5 mg/mL. The morphology was then characterized using TEM, to establish the uniform coating of silica over the nanoparticles.

Subsequently, 50 mg mal-PEG silane was added to 1 mL of 8.5 mg/mL silica-coated UCNP suspension in water, ultrasonicated for 1 min and kept under shaking for 3 h. The mixture was centrifuged in an Eppendorf microfuge at 15,000 g for 30 min. The precipitate was then washed with water, redispersed in 1 mL of phosphate buffered saline (PBS, comprising 0.14 M KCl, 50 mM phosphate and pH 7.4), and ultrasonicated to yield a homogeneous suspension.

Silica coated UCNP dispersion is stable for several hours and partly precipitates within a couple of days. However these UCNPs easily redisperse and show nearly 100% photoluminescence even after at least 4–5 months' storage.

2.4. Conjugation of ofloxacin with bovine serum albumin (BSA)

Ethylenediamine (200 μL) was added to 10 mL of 50 mg/mL BSA solution in PBS. The pH of the solution was adjusted to 7.4, then 100 mg of EDC and 100 mg sulfo-NHS were added and the mixture was stirred for 2 h. Ethylenediamine modified BSA (BSA-NH_2) was purified on a desalting PD10 column (GE-Biosystems). BSA-NH_2 (~15 mL) was then mixed with 150 μL of 1 M ofloxacin in 1 M NaOH solution. After adjusting the pH to 7.4, 100 mg of EDC plus 100 mg sulfo-NHS were added to BSA-NH_2 mixture and the conjugation reaction has been carried out for 2 h under stirring. In the next step, the ofloxacin-BSA conjugate was purified on a PD10 desalting column and effective conjugation was tested by dot blot analysis [37]. Drops of BSA control solution (6 mg/mL in PBS) and drop of ofloxacin-BSA solutions (6 mg/mL in PBS) were absorbed onto nitrocellulose membrane. The membrane was then blocked in blocking buffer (1% (w/v) casein in PBS buffer with 0.1% (v/v) Tween 20 added (PBST)) for 1 h with gentle agitation on an orbital shaker. Then the membrane was washed 3 times with blocking buffer. The nitrocellulose membrane was then incubated with rabbit anti-ofloxacin primary antibodies for 1 h. The membrane was washed 3 times with PBST and incubated with anti-rabbit-HRP secondary antibodies. The bound antibodies were visualised by enhanced chemiluminescence (ECL) after adding ECL substrate (Pierce ECL Western Blotting Substrate – Product 32209). The dot blot image has been captured by placing the ECL substrate added membrane in a Syngene G-Box imager machine, adopting the G:BOX Chemi XX6 Genesys software.

2.5. Anti-ofloxacin conjugation with silica coated UCNPs

One mL of anti-ofloxacin IgG (~2.5 mg/mL) was mixed with 280 μL of 10 mM TCEP and incubated for a period of 1.5 h at 37 °C. This process allows cleavage of the antibody to obtain reduced half antibodies for exposing the –SH linkages to conjugate with the maleimide groups on the UCNPs. The reduced antibody solution was mixed with 1 mL mal-PEG-silane modified UCNPs and the pH was adjusted to 7 by adding PBS.

2.6. Competitive ofloxacin assay

A 96 well polystyrene plate was incubated with BSA-ofloxacin (50 μL of 8 mg/mL per well) at 4 °C for 24 h before adding 1% (w/v) casein and 10 mg/mL BSA in PBST blocking buffer at 200 μL per well. The plate was incubated with this blocking buffer for 1 h and then washed with PBST four times. A series of ofloxacin and sulfamethazine (control) dilutions ranging from 0.1 mM to 10 nM were prepared in 50 mM HEPES buffer (pH 7.4). Anti-ofloxacin-UCNPs were then mixed with each concentration of antibiotics (ofloxacin or sulfamethazine) in HEPES buffer and incubated for 30 min at room temperature. Subsequently each antibiotic-antiofloxacin-UCNP mixture (ofloxacin- antiofloxacin-UCNPs as well as sulfamethazine-antiofloxacin-UCNPs) was placed in the individual well in the ofloxacin modified plate for 30 min. The plate was then washed with PBS buffer and the photoluminescence was measured on a BMG LabTech plate reader by exciting bound UCNPs using a 976 nm diode laser and using a 520 nm emission filter.

3. Results and discussion

The formation of particles at different times after reaching the reaction temperature of 300 °C was studied using TEM of the nanoparticles in solutions taken at 40, 60, 90 and 120 min, and the images of particles in those solutions are presented Fig. 1(A–D). The histograms corresponding to each image depicting the particle size distribution are reported in Fig. S1.

A mean particle size of around 52 nm was observed as the reaction time was increased to 120 min while the mean size was around 22 nm at 90 min reaction time. It was observed that the particles showed homogeneous growth with little clustering or agglomeration as evident from the TEM. The variation in mean particle size with time after the optimum temperature was reached is shown in Fig. 1E. The data indicate an increased rate of growth of particles as time proceeds. The uniform and exponential nucleation and growth process from particle size of 12.7 ± 1.5 nm (at reaction time of 40 min) to 21 ± 1.6 nm (at reaction time of 90 min) was seen, but as the reaction time was increased from 90 to 120 min, a sharp increase in particle size (52 ± 3.7 nm) was observed. In our experiment, 1-octadecene (ODE) was used as the primary organic solvent to provide a high-temperature environment based on its high boiling point, while oleic acid acts as a surfactant and controls the crystal growth of the UCNPs by coordinating to the particle surface and forming a hydrophobic layer. Oleic acid acts as the coordinating ligand thus forms a uniform coating layer on the UCNPs as a result of the formation of a lanthanide-oleate complex initially as a shell. The oleate ligands adsorbed on the surface makes it hydrophobic and help to disperse in hydrophobic organic solvents [38]. Thus, during the reaction process, the surfactant plays two roles: (1) capping the surface of UCNPs to prevent them from aggregation (2) controlling the growth of the nanoparticles by a selective absorption effect [39].

Fig. S2 shows the homogeneous suspension obtained after a reaction time of 120 min which is opaque due to non-absorptive light scattering by the UCNPs. Under 976 nm laser illumination the UCNPs showed a green visible light emission. The upconversion PL spectra of particles in solution obtained at different reaction times are presented in Fig. 2. Upconversion emission peaks were clearly observed from sample obtained from reaction times of 40 min and longer. An increase in the total PL count was observed with longer reaction times. The three emission peaks in the spectra were attributed to $^2H_{11/2}$ to $^4I_{15/2}$ (around 520 nm green emission), $^4S_{3/2}$ to $^4I_{15/2}$ (around 541 nm-green emission) and $^4F_{9/2}$ to $^4I_{15/2}$ (around 653 nm-red emission) transition of the Er^{3+} ions in the nanoparticles, with the most intense green emission observed at 541 nm. The integrated PL intensity and the contribution of green emissions to this were expected to be greater for particles of larger size. The ratio of

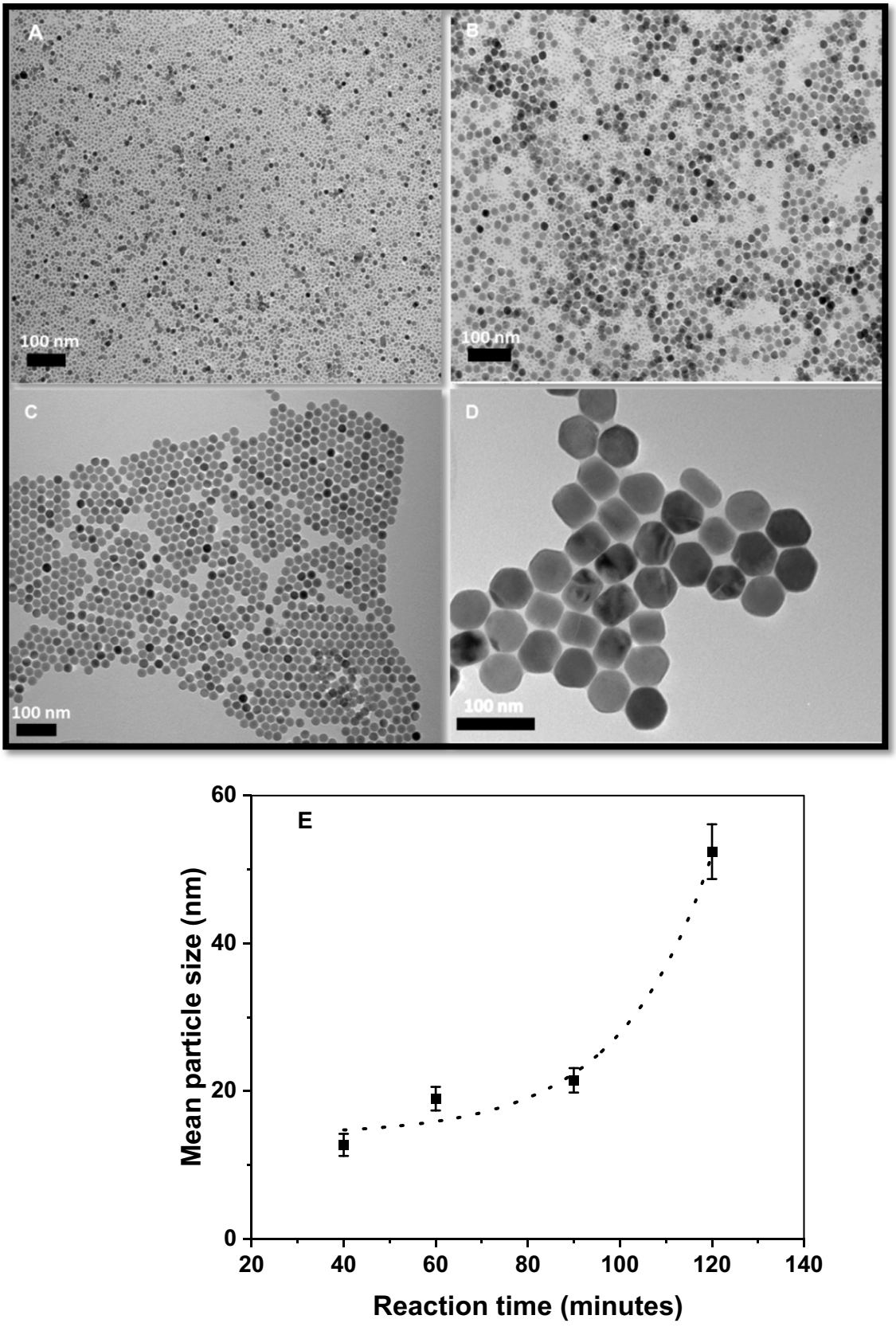

Fig. 1. TEM images showing hexagonal UCNP formed in solution after different reaction times from the optimum temperature of 300 °C. (A), 40 min; (B), 60 min; (C), 90 min; (D), 120 min; (E), Variation in average particle size with reaction time after the optimum reaction temperature was reached.

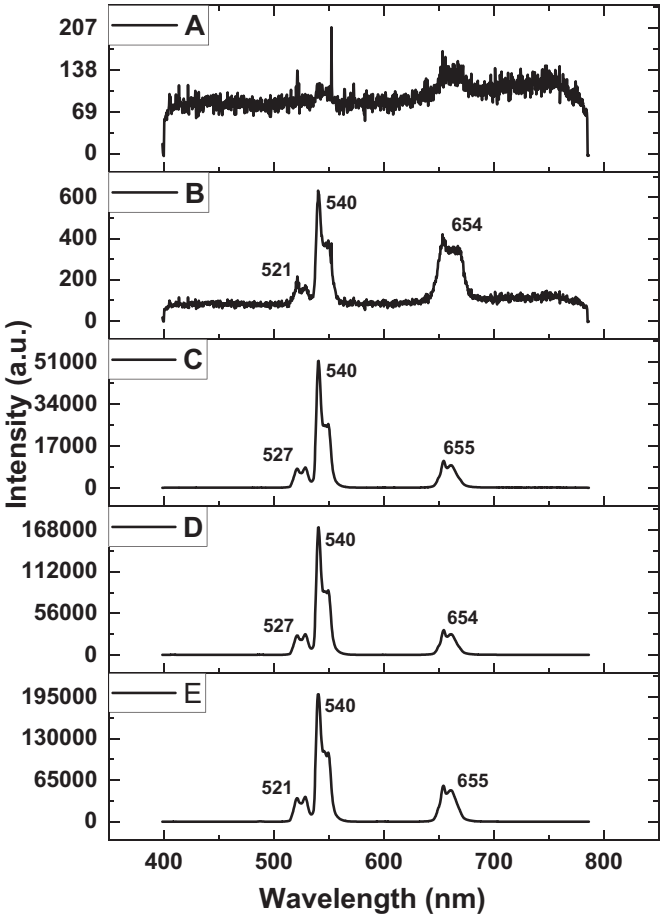

Fig. 2. Photoluminescence emission spectra showing formation of hexagonal UCNPs with reaction time at 300 °C. Once 300 °C had been reached spectra were recorded at: (A), 20 min; (B), 40 min; (C), 60 min; (D), 90 min; (E), 120 min.

integrated PL intensities in the green (512–560 nm) and red (637–674 nm) wavelength range calculated from the spectra for different particles sizes is defined as the G/R ratio. It is clear that the intensity of green emission relative to red increases with mean particle size. The G/R ratio and integrated green intensity vs mean particle size is presented in Fig. 3 and showed a substantial increase for 120 min reaction time. The increase showed a nearly linear trend and correlated to the formation of larger particles shown in Fig. 3.

This increase in PL with particle size is due to the decrease in specific surface area of the particles which is favourable for reducing non-radiative relaxation pathways [9]. In addition, the larger nanocrystals possess a relatively decreased number of surface quenching sites and thus enhance the up-conversion luminescence by reducing the non-radiative energy transfer assisted PL decay process of the luminescent lanthanide ion [40].

It was noticed that the percentage contribution from integrated green luminescence was directly proportional to the mean particle size and the particles showed 74.4% of the total integrated luminescence emission as the particle size of 52 nm was reached after 120 min reaction time. The variation in G/R values observed in our experiments were concordant with the results by Zhao et al. [8] where G/R luminescence intensity ratio increases, as the particle size is varied from 6 nm to 45 nm in both cubic and hexagonal $NaYF_4$ phases. Sample with higher particle size was utilised in our research discussed below for ofloxacin detection due to their higher integrated green photoluminescence.

The particles obtained after 120 min reaction time were then coated with silica in order to make them hydrophilic, biologically non-toxic and

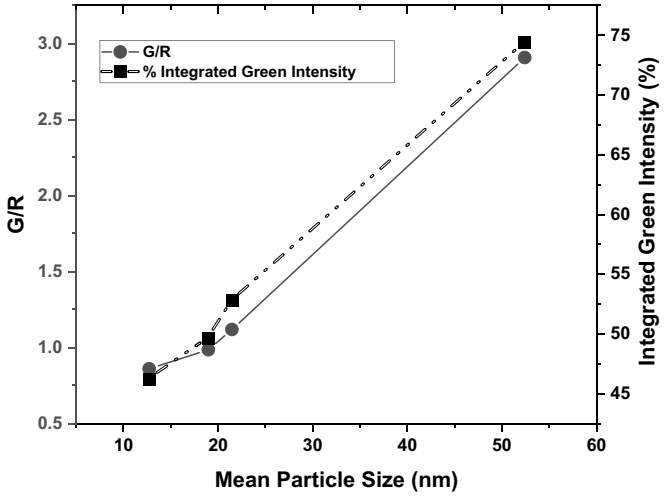

Fig. 3. Variation in ratio of integrated green (512–560 nm) to red (637–674 nm) (G/R) and percentage integrated green intensity vs mean particle size.

to enable ease of functionalisation. Oleic acid capped $NaYF_4/Yb^{3+}/Er^{3+}$ UCNPs dispersed in cyclohexane were added to an IGEPAL-cyclohexane mixture which acted as a reverse micro-emulsion for polymerisation of the TEOS precursor, while ammonia acted as a catalyst, during the silica-coating procedure. This brought about steady growth of the silica shell, thus resulting in uniform silica-coated UCNPs [41]. The silica coating also led to less aggregation thus maintaining the homogeneity of the system while subsequent mal-PEG-silane addition provided suitable thiol reactive sites for antibody attachment. An additional advantage of the PEG-linker was prevention of agglomeration with well-maintained monodispersity [42] and reduction in non-specific binding [43]. TEM images of the silica coated hexagonal nanoparticles are shown in Fig. 4.

The particle size distribution analysis of silica coated UCNPs (Supplementary information Fig. S3) showed a broader distribution as compared to the uncoated UCNPs. It was observed that an average particle size of around 61.1 ± 4 nm was observed for silica-coated particles while a mean value of 52 ± 3.7 nm was indicated for uncoated particles. This amounted to a silica coating thickness of ~10 nm on the UCNPs.

A comparison of the PL spectra of silica coated particle and the bare UCNPs in cyclohexane is presented in Fig. 5.

The reduction in the G/R emission ratio (G/R = 1.42), might be due to the non-radiative decay in the presence of the silica coating which quenches the green emission. This quenching is due to the -OH groups within the silica coating.

The X-ray diffraction pattern of the sample with reaction time 120 min is shown in Fig. S4. Cubic phase was observed even for the sample with 90 min reaction time (data not shown), while the sample with 120 min reaction time showed highly crystalline pure hexagonal phase as per JCPDS 16-0334. The crystal lattice parameters were found to be $a = b =$ 5.9835 Å, $c = 3.5121$ Å ($\alpha = \beta = 90°$; $\gamma = 120°$) with the space group P63/m, for the phase pure hexagonal sample.

A competitive assay was established in order to use the surface modified anti-ofloxacin-UCNP conjugate for the detection of ofloxacin on plate in a fluorescence plate-reader. In the process of optimising the competitive assay, BSA was conjugated with ofloxacin using EDC/sulfo-NHS followed by adsorption of ofloxacin-BSA conjugate on plate wells. Ofloxacin-BSA conjugate formation was tested by dot blot analysis (Fig. 6). The chemiluminescence observed on the ofloxacin-BSA conjugate showed effective bioconjugation of ofloxacin molecules to BSA.

The hydrophilised UCNPs, adopting the procedure of silica coating, were used for production of anti-ofloxacin IgG-UCNP conjugate. Coating the plate wells with ofloxacin-BSA conjugate allows a competitive assay to be effective since the coating allows capture of free anti-ofloxacin IgG-

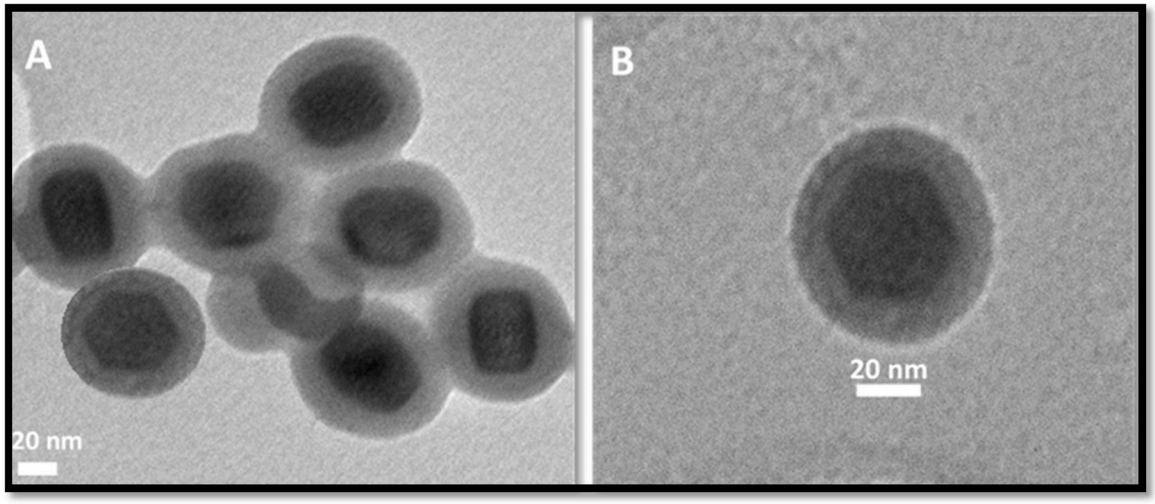

Fig. 4. TEM of silica coated upconversion nanoparticles showing uniform silica coating on the UCNPs. (A), Uniform silica coating on UCNPs; (B), Enlarged image of silica-coated hexagonal shaped UCNP.

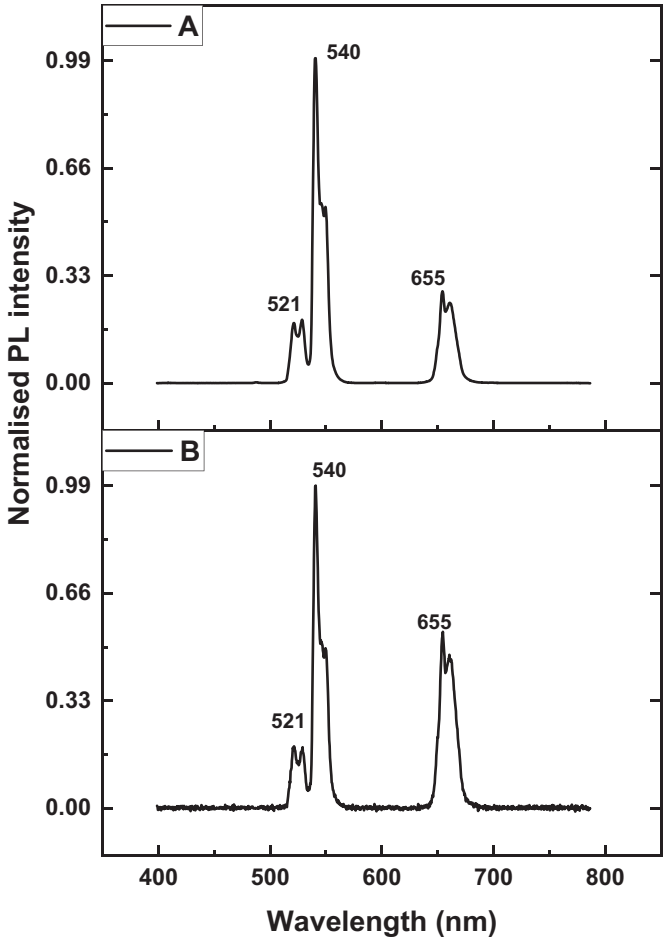

Fig. 5. Photoluminescence emission spectra of bare and silica coated UCNPs (data normalised to 540 nm peak intensity). Spectra were recorded on an Ocean Optics QE Pro spectrofluorimeter using 976 nm laser excitation. (A), Bare UCNPs; (B), Silica coated UCNPs.

UCNP conjugate on the plate. Fig. 7 shows the assay over a range of ofloxacin from 0.1 mM to 10 nM.

The calibration curve showed good linearity with an R^2 of 0.9904,

Fig. 6. Dot blot images of BSA and ofloxacin-BSA conjugate. (A), control BSA; (B), ofloxacin-BSA conjugate. Images were captured by standard western blot procedure with anti-ofloxacin rabbit IgG and anti-rabbit HRP-IgG. The bound HRP-IgG were visualised by enhanced chemiluminescence (ECL).

which is a minimal variation when a linear regression fit was performed for the ofloxacin plot. Overall, the reported method has the advantage compared to ELISA because of the less steps involved. Our method comprises simply addition of ofloxacin to the anti-ofloxacin IgG-UCNP conjugate, then addition to the plate precoated with ofloxacin antigen, followed by a brief incubation and plate wash before readout. The selectivity of anti-ofloxacin-UCNPs depends on selectivity of anti-ofloxacin antibodies. So as the interference experiment (control experiment), the anti-ofloxacin-UCNP conjugate was tested against sulfamethazine antibiotic. The results show no response of assay to

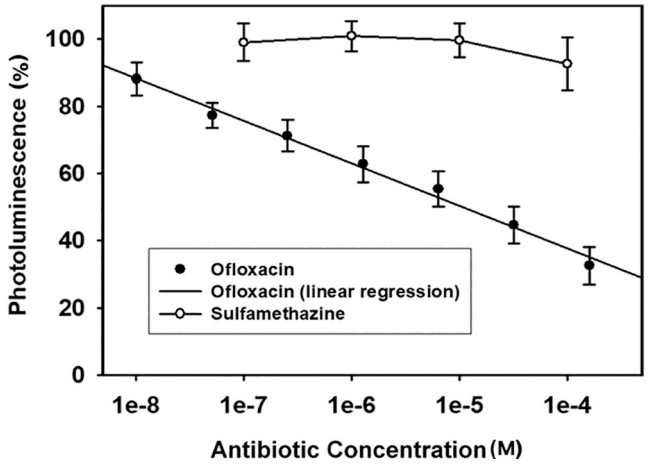

Fig. 7. UCNP photoluminescence competitive assay calibration curve. Data are mean ± SD (n = 3).

sulfamethazine, which indicates the specificity of the anti-ofloxacin-UCNP conjugate (Fig. 7). The assay format could be directly adapted for detection of other biomarkers, both small molecule such as ofloxacin and larger biomolecules such as proteins. Thus, the novelty of the work includes single step ofloxacin detection using ofloxacin modified 96 well plates and highly effective detection using UCNPs due to the high signal/noise ratio. The competitive assay developed in the present study, adopting silica coated hydrophilised UCNPs, demonstrates ofloxacin detection down to approximately 10 nM. It is expected that the use of bioreceptors such as affimers (adhirons) and aptamers having lower dissociation constant (K_D) could lower the detection limit, which could be a future perspective. Previously reported work regarding using materials such as ZrO_2 used for coating particles such as $CsPbBr_3$ [44] where the application comes as white light emitting diodes, may be tried effectively in the process of hydrophilising the UCNPs too. The uniformity of coating and less efficiency in quenching of the PL should be considered.

4. Conclusion

Highly photoluminescent uniformly sized β-$NaYF_4$/Yb^{3+}/Er^{3+} up-conversion nanoparticles (UCNPs) were prepared by a solvothermal method at 300°C under an Ar atmosphere. The variation in particle size and photoluminescence with respect to time and temperature was studied. It was shown that the percentage of green emission was higher in larger UCNPs when integrated fluorescence was considered. The UCNPs dissolved in cyclohexane were made hydrophilic by incorporating a uniform silica coating in order to make the particles suitable for bio-applications. The hydrophilic silica-coated particles were modified using maleimide-PEG-silane in order to introduce maleimide groups. The hydrophilic maleimide modified UCNPs were conjugated with reduced IgGs directed against the veterinary antibiotic, ofloxacin. A rapid competitive assay was produced for detection of low concentrations of ofloxacin, with a minimum concentration of ~10 nM which may be useful for environmental monitoring; the assay format could easily be adapted for other analytes for which an antibody is available. The future prospects include the use of affimers or aptamers in the place of antibodies in order to lower the detection limit.

CRediT authorship contribution statement

Corresponding Author, **Padmaja Parameswaran Nampi**-Conceptualization, Experimental executions and characterization, Original manuscript preparation, Fellowship. **Alexander Vakurov**-Experimental executions and discussions; **Sikha Saha**-Reviewing; **Gin Jose**-Supervision, Reviewing, Funding. **Paul A. Millner**-Supervision, Experimental facilities, Resources, Reviewing and Funding.

Declaration of competing interest

The authors declare that they have no known competing financial interests or personal relationships that could have appeared to influence the work reported in this paper.

Acknowledgement

The Corresponding Author Padmaja Parameswaran Nampi (PPN) has received funding from the European Union-Horizon 2020 Framework Programme – H2020 Marie Skłodowska-Curie Actions - Marie Skłodowska-Curie Individual Fellowship for Experienced Researchers under the Grant Agreement No. RECORDER-707297 to carry out this work. Alexander Vakurov was funded by the UK Natural Environment Research Council (NERC, UK) (Grant No. NE/N007581/1). The authors also would like to thank Engineering and Physical Sciences Research Council, UK (EPSRC, UK) for the financial support through the research grants (EP/M015165/1 and EP/T004711/1). The authors acknowledge the Astbury Biostructure Laboratory, The Astbury Centre for Structural Molecular Biology, University of Leeds for the Transmission electron microscopy facilities for this study.

Appendix A. Supplementary data

Supplementary data to this article can be found online at https://doi.org/10.1016/j.bioadv.2022.212763.

References

[1] R. Scheps, Prog. Quantum Electron. 20 (1996) 271–358.
[2] F. Auzel, Chem. Rev. 104 (2004) 139–174.
[3] F. Wang, X. Liu, Chem. Soc. Rev. 38 (2009) 976–989.
[4] F. Wang, D. Banerjee, Y. Liu, X. Chen, X. Liu, Analyst 135 (2010) 1839–1854.
[5] J. Suyver, A. Aebischer, D. Biner, P. Gerner, J. Grimm, S. Heer, K. Kramer, C. Reinhard, H.G. Udel, Opt. Mater. 27 (2005) 1111–1130.
[6] J. Shan, M. Uddi, N. Yao, Y. Ju, Adv. Funct. Mater. 20 (2010) 3530–3537.
[7] S. Schietinger, L.D.S. Menezes, B. Lauritzen, O. Benson, Nano Lett. 9 (2009) 2477–2481.
[8] J. Zhao, Z. Lu, Y. Yin, C. McRae, J.A. Piper, J.M. Dawes, D. Jin, E.M. Goldys, Nanoscale 5 (2013) 944–952.
[9] F. Wang, J. Wang, X. Liu, Angew. Chem. Int. Ed. 49 (2010) 7456–7460.
[10] G. Liu, Chem. Soc. Rev. 44 (2015) 1635–1652.
[11] H. Song, L. Yu, S. Lu, T. Wang, Z. Liu, L. Yang, Appl. Phys. Lett. 85 (2004) 470–472.
[12] G.J. De, W.P. Qin, J. Zhang, J.S. Zhang, Y. Wang, C.Y. Cao, Y. Cui, Solid State Commun. 137 (2006) 483–487.
[13] K.W. Krämer, D. Biner, G. Frei, H.U. Güdel, M.P. Hehlen, S.R. Lüthi, Chem. Mater. 16 (2004) 1244–1251.
[14] J.F. Suyver, J. Grimm, K.W. Krämer, H.U. Güdel, J. Lumin. 114 (2005) 53–59.
[15] S. Heer, K. Kömpe, H.U. Güdel, M. Haase, Adv. Mater. 16 (2004) 2102–2105.
[16] J.H. Zeng, J. Su, Z.H. Li, R.X. Yan, Y.D. Li, Adv. Mater. 17 (2005) 2119–2123.
[17] H.X. Mai, Y.W. Zhang, R. Si, Z.G. Yan, L.D. Sun, L.P. You, C.H. Yan, J. Am. Chem. Soc. 128 (2006) 6426–6436.
[18] A. Aebischer, S. Heer, D. Biner, K. Krämer, M. Haase, H.U. Güdel, Chem. Phys. Lett. 407 (2005) 124–128.
[19] J. Zhou, Z. Liu, F.Y. Li, Chem. Soc. Rev. 41 (2012) 1323–1349.
[20] P.D. Howes, R. Chandrawati, M.M. Stevens, Science 346 (2014) 1247390.
[21] C.H. Liu, H. Wang, X. Li, D. Chen, J. Mater. Chem. 19 (2009) 3546–3553.
[22] G. Chen, H. Qui, P.N. Prasad, X. Chen, Chem. Rev. 114 (2014) 5161–5214.
[23] S. Cui, H. Chen, Y. Gu, J. Phys. Conf. Ser. 277 (2011), 012006.
[24] P.L.A.M. Corstjens, S. Li, M. Zuiderwijk, K. Kardos, W.R. Abrams, R.S. Niedbala, H. J. Tanke, IEEE Proc. Nanobiotechnol. 152 (2005) 64–72.
[25] S. Li, H. Feindt, G. Giannaras, R. Scarpino, S. Salamone, R.S. Niedbala, Proc. SPIE Int. Soc. Opt. Eng. 4890 (2002) 100–109.
[26] G. Yi, H. Lu, S. Zhao, Y. Ge, W. Yang, D. Chen, L.H. Guo, Nano Lett. 4 (2004) 2191–2196.
[27] T. Soukka, T. Rantanen, K. Kuningas, Ann. N. Y. Acad. Sci. 1130 (2008) 188–200.
[28] K. Watanabe, K. Numata-Watanabe, S. Hayasaka, Ophthalmic Res. 33 (2001) 136–139.
[29] N. Kurokawa, K. Hayashi, M. Konishi, M. Yamada, T. Noda, Y. Mashinia, Jpn. J. Ophthalmol. 46 (2002) 586–589.
[30] W. Liu, Y. Guo, H. Li, M. Zhao, Z. Li, B. Li, Spectrochim. Acta A Mol. Biomol. Spectrosc. 137 (2015) 1298–1303.

[31] Z. Tong, Y. Bianfei, T. Wanjin, Z. Haixia, Spectrochim. Acta A Mol. Biomol. Spectrosc. 148 (2015) 125–130.
[32] C. Immanuel, A.K. Hementh Kumar, J. Chromatogr. B Biomed. Sci. Appl. 760 (2001) 91–95.
[33] A.O. Alnajjar, J. Liq. Chromatogr. Relat. Technol. 36 (2013) 2687–2697.
[34] O. Plohl, S. Kralj, B. Majaron, E. Fröhlich, M. Ponikvar-Svet, D. Makovec, D. Lisjak, Dalton Trans. 46 (2017) 6975–6984.
[35] Y. Wei, F. Lu, X. Zhang, D. Chen, Chem. Mater. 18 (2006) 5733–5737.
[36] R.A. Jalil, Y. Zhang, Biomaterials 29 (2008) 4122–4128.
[37] J.V. Rushworth, A. Ahmed, H.H. Griffiths, N.M. Pollock, N.M. Hooper, P.A. Millner, Biosens. Bioelectron. 56 (2014) 83–90.
[38] X. Xue, S. Uechi, R.N. Tiwari, Z. Duan, M. Liao, M. Yoshimura, T. Suzuki, Y. Ohishi, Opt. Mater. Exp. 3 (2013) 989–999.
[39] M. Ding, D. Chen, Lanthanide ions doped upconversion nanomaterials: synthesis, surface engineering, and application in drug delivery, in: A.M. Holban, A. M. Grumezescu (Eds.), Nanoarchitectonics for Smart Delivery and Drug Targeting, William Andrew Applied Science Publishers, 2016, pp. 227–260.
[40] F. Wang, Y. Han, C.S. Lim, Y. Lu, J. Wang, J. Xu, H. Chen, C. Zhang, M. Hong, X. Liu, Nature 463 (2010) 1061–1065.
[41] V. Muhr, S. Wilhelm, T. Hirsch, O.S. Wolfbeis, Acc. Chem. Res. 47 (2014) 3481–3493.
[42] Q. Xiao, W. Bu, Q. Ren, S. Zhang, H. Xing, F. Chen, M. Li, X. Zheng, Y. Hua, L. Zhou, W. Peng, H. Qu, Z. Wang, K. Zhao, J. Shi, Biomaterials 33 (2012) 7530–7539.
[43] A. Sedlmeier, H.H. Gorris, Chem. Soc. Rev. 44 (2015) 1526–1560.
[44] Q. Mo, C. Chen, W. Cai, S. Zhao, D. Yan, Z. Zang, Laser Photonics Rev. 15 (2021) 2100278.